Scientific Research Publishing

Journal of Geoscience and Environment Protection, 2023, 11, 290-315
https://www.scirp.org/journal/gep
ISSN Online: 2327-4344
ISSN Print: 2327-4336

Quantitative and Comprehensive Prediction of Shale Oil Sweet Spots in Qingshankou Formation, Songliao Basin

Tiantian Wu[1*], Xin Bai[2,3], Fei Shang[4], Haiyan Zhou[4], Lan Wang[4], Xuexian Zhou[4], Zhi Zhong[1], Zhi Yang[4], Jinyou Zhang[5], Xinyang Cheng[3], Peiyu Zhang[6], Ruiqian Chen[2,3]

[1]Laboratory Information and Internet, China University of Geosciences, Wuhan, China
[2]China University of Petroleum (Beijing), Beijing, China
[3]State Key Laboratory of Oil and Gas Resources and Exploration, Beijing, China
[4]Research Institute of Petroleum Exploration & Development, Beijing, China
[5]Daqing Oilfield Company, Daqing, China
[6]Qingdao Liquefied Natural Gas Co., Ltd., Qingdao, China
Email: *wtiantian2016@cug.edu.cn

How to cite this paper: Wu, T. T., Bai, X., Shang, F., Zhou, H. Y., Wang, L., Zhou, X. X., Zhong, Z., Yang, Z., Zhang, J. Y., Cheng, X. Y., Zhang, P. Y., & Chen, R. Q. (2023). Quantitative and Comprehensive Prediction of Shale Oil Sweet Spots in Qingshankou Formation, Songliao Basin. *Journal of Geoscience and Environment Protection, 11,* 290-315.
https://doi.org/10.4236/gep.2023.115018

Received: April 10, 2023
Accepted: May 28, 2023
Published: May 31, 2023

Abstract

The mud shale of Qingshankou Formation in Songliao Basin is the main rock source and contains rich shale oil resources. The successful development of shale oil depends on evaluating and optimizing the "sweet spots". To accurately identify and optimize the favorable sweet spots of shale oil in Qingshankou Formation, Songliao Basin, the original logging data were preprocessed in this paper. Then the thin mud shale interlayer of Qingshankou Formation was identified effectively by using the processed logging data. Based on the artificial neural network method, the mineral content of mud shale in Qingshankou Formation was predicted. The lithofacies were identified according to the mineral and TOC content. Finally, a three-dimensional (3-D) model of total organic carbon (TOC), vitrinite reflectance (Ro), mineral content, and rock of Qingshankou Formation in Songliao Basin was established to evaluate and predict the favorable sweet spots of shale oil in the study area. The results show that there are a lot of calcareous and siliceous thin interlayers in Qingshankou Formation, and TOC content is generally between 2% and 3%. Ro is the highest in Gulong sag, followed by Sanzhao sag. The lithofacies mainly consists of felsic shale and mixed shale, mainly in the first member of Qingshankou Formation. Comprehensive analysis shows that shale oil development potential is enormous in the eastern part of Sanzhao Sag and the northern part of Gulong Sag.

Keywords

Songliao Basin, Qingshankou Formation, Shale Oil, Sweet Spot, Artificial Neural Network

1. Introduction

As the difficulty of finding conventional oil and gas resources increases year by year, the proportion of unconventional oil and gas in oil and gas exploration is increasing. Shale oil resources with high abundance and large area distribution have become a hot target of oil and gas exploration and development (Allix et al., 2010; Ryder et al., 2003). In recent years, great breakthroughs have been made in shale oil exploration in central Sichuan, Songliao, Ordos, Junggar and Qaidam Basins, and considerable reserves of shale oil resources have been discovered successively, especially in the Qingshankou Formation of Songliao Basin. Effective prediction of sweet spot is a fundamental prerequisite for successful shale oil development (Holditch, 2013).

Shale oil is an essential unconventional oil and gas resource (Holditch, 2013; Tourtelot, 1964), composed of nano-micron pores and fractures in source rock (Huang et al., 2013). In the past 20 years, shale oil has made significant progress in oil and gas exploration and engineering development. Since the commercial development of shale oil and gas, it has made a rapid breakthrough in North America, South America, Australia, Europe, Asia, and Africa. It has become a kind of fossil energy with considerable reserves (Zou et al., 2016). In recent years, great breakthroughs have been made in shale oil exploration in Sichuan, Songliao, Ordos, Junggar, and Qaidam Basins in China, and considerable reserves of shale oil resources have been discovered successively, especially in the Qingshankou Formation of Songliao Basin. Effective prediction of sweet spots is a fundamental prerequisite for successful shale oil development. The great success of shale oil development in the United States has profoundly affected the international energy pattern and has a profound impact on the global energy industry.

Songliao Basin is a large meso-Cenozoic continental sedimentary Basin superimposed on the Paleozoic base in eastern China. There are several sets of source rocks with vibrant organic matter and rich shale oil resources (Tian et al., 1992). Through years of exploration practice, Zhang et al. (2021) believed that two large-scale transgressive events occurred during the depositional period of Qingshankou Formation (Cenomanian Period) and Nenjiang Formation (Turonian Period) in the Songliao Basin, forming two sets of semi-deep lakes—Deep lacustrine mud shale deposits develop deep lacustrine organic-rich fine-grained sedimentary rocks, which provide a material basis for the Formation of shale oil. Cui et al. (2020) pointed out that the Qingshankou Formation has high-mature shale oil with considerable geological resources and has the advantages of "three highs and one low" (high maturity, high gas-oil ratio, high-pressure coefficient, and low crude oil density). In addition, the high content of clay minerals and low content of carbonate and felsic minerals also provides favorable conditions for its shale oil hydraulic fracturing (Cui et al., 2020).

Based on a large number of well logging data, limited core experimental data, and two sets of seismic interpretation layer in Formation, combined with artificial neural network method, the mineral content of Qingshankou Formation mud shale the lithofacies are identified. Determine sweet spot areas from both geological and engineering considerations. The geological sweet spot was determined by the abundance of organic matter, oil content, maturity, and total organic carbon (TOC), and the engineering sweet spot was analyzed by the content of three minerals, siliceous, clay, and carbonate rock, and a green spot in the Songliao Basin was established. The three-dimensional structural and attribute model of the Qingshankou Formation can quantitatively determine the shale oil sweet spots and promote the efficient exploration and development of shale oil in the Songliao Basin.

2. Geological Setting

The tectonic evolution of the study area mainly went through 4 stages: fault depression stage (Jurassic depositional period), fault depression stage (Denglouku Formation depositional period), depression stage (Quantou Formation-Nenjiang Formation depositional period) and shrinkage uplift stage (late Nenjiang to Nenjiang Formation) Cenozoic). There are Jurassic, Cretaceous and Paleogene clastic sedimentary strata developed in the Basin. Among them, the Upper Cretaceous Qingshankou Formation developed a set of semi-deep lacustrine and deep lacustrine organic-rich mud shale sedimentary strata, and the thickness distribution is relatively stable, close to 1000 m, the horizontal distribution area reaches (10 - 18) × 10^4 km^2 (**Figure 1**).

The Qingshankou Formation mud shale was formed in the Semi-deep water—deep water lacustrine reduction environment affected by transgression, and formed a large area of deep lacustrine dark mudstone in the green depositional period of a wide range of water bodies (Shang et al., 2022). The most important source rock is in the Songliao Basin. A large number of thin interlayers are developed in the Qingshankou Formation mudstone (Zhang et al., 2021), which can be subdivided into calcareous interlayers (ostracods) and sandy interlayers (siltstone, fine sandstone). Among them, the central depression area is almost entirely deposited with extremely thick organic-rich shale, with a thickness of 90 - 270 meters and an area of more than 3 × 10^4 km^2. After the mud shale is deposited, the structure is stable, and it has not experienced major uplifting and denudation and major fault damage (Passey et al., 1990), which provides important geological conditions for the Formation and preservation of shale oil.

3. Data and Methodology

3.1. Available Data

The primary available data consist of 661 sets of core data, abundant wireline

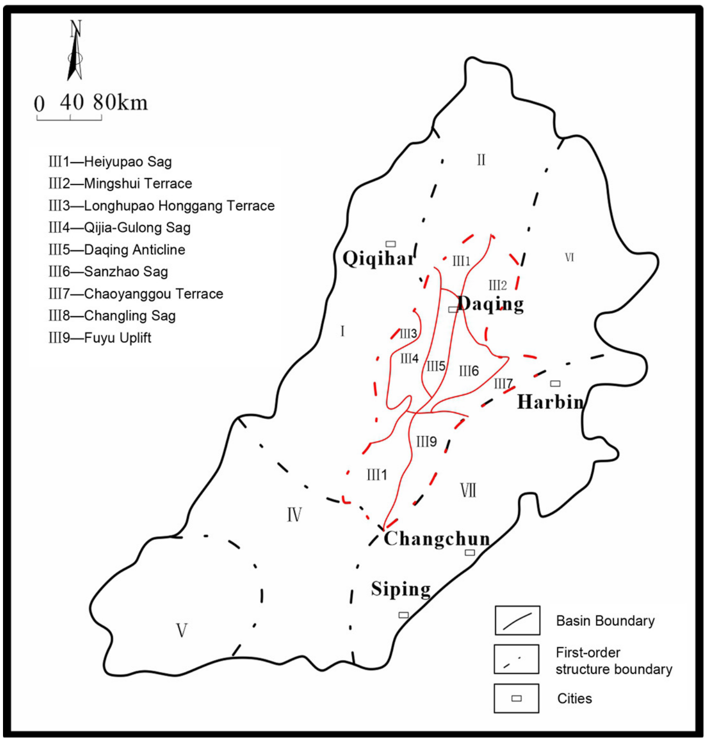

Series	Formation		Segment	Thickness/m	Seismic reflection interface	Sediment system	Reservoir
Quaternary		Q		0~143			
Neogene	Taikang	Nt		0~165			
Paleogene	Da'an	Nd		0~123			
Upper Cretaceous	Yi'an	Ey		0~260	T_{02}		
	Mingshui	K_2m	2	0~381		Delta/shallow lake	
			1	0~243			
	Sifangtai	K_2m		0~413	T_{03}	Alluvial fan/river	
	Nengjiang	K_2n	5	0~355			
			4	0~290			Heidi Temple
			3	50~177		Delta/shallow lake	
			2	80~253			
			1	27~222	T_1		Saertu
	Yaojia	K_2y	2.3	50~150		Shallow lake/delta/river	
			1	10~80	T_1^1		Putaohua
	Qingshankou	K_2QN	3	50~552		Delta/shallow lake/semi-deep lake	Gaotaizi
			2				
			1	25~164	T_2		
Lower Cretaceous	Quantou	K_2q	4	0~128			Fuyu
			3	0~692		Delta/river/shallow lake	Yangda chengzi
			2	0~479			
			1	0~855	T_3		

Figure 1. A plane structure diagram of Songliao Basin (left) (modified according to document (Liu et al., 2021) and the stratigraphic division map of Songliao Basin (right).

logs, two 3-D seismic volumes, and they were used for inter-well small zone correlation, thin interlayer recognition, vitrinite reflectance (Ro) calculation, total organic carbon (TOC) prediction, and mud shale lithofacies identification. Due to the large study area, wide logging data sources, and long acquisition time span, original well logging data needed to be preprocessed before use.

3.2. Normalization

Deep lateral resistivity (LLD) and acoustic (AC) overlapped each other in the middle and lower part of Qing 3 member and most of the middle and upper part of Qing 2 member, and nearly covered at the top of Quantougou Formation. The two curves were normalized by translating the deep lateral resistivity and acoustic time difference curves so that they overlapped or almost overlapped in the middle and lower part of Qing 3 member and the middle and upper part of Qing 2 member. Then the density (RHOB) and neutron porosity (NPHI) curves were normalized using AC and LLD as reference. Density logging basically overlapped with LLD and AC in the middle and lower parts of Qing 3 member, the middle and upper parts of Qing 2 member, and the upper part of Quantougou Formation, while NPHI is similar to DEN. The positions of the middle and lower part of Qing 3 member, the middle and upper part of Qing 2 member, and the upper part of Quantougou Formation basically overlapped with the deep lateral resistivity and acoustic time difference. Finally, the natural gamma (GR) was normalized.

Then stratified the strata according to logging data and established the stratigraphic framework of Qingshankou Formation in the whole Basin.

3.3. Identification Thin Interlayers

Thin interlayers usually resulted in peaks in LLD curve, as well as AC and DEN peaks. Compared with the deep investigate induction log (ILD), the response of LLD to thin interlayer was more obvious in the study area, and the thin interlayer cannot be identified effectively.

Compared with the logging curves of ILD, AC, and DEN, the sharp peak of LLD corresponded best to thin interlayers. Therefore, this paper mainly identifies thin intercalation based on the sharp peak of LLD. The specific steps are as follows: The envelope algorithm is used to automatically calculate the difference between each peak and the envelope (peak height), and then calculate the width of each peak (peak width). Narrow and high peaks are screened by the ratio of peak height to peak width. Finally, calcareous intercalation and sandy intercalation are distinguished according to the DEN value (Figure 2). In order to calculate the peak height and peak width better, this article through to the envelope

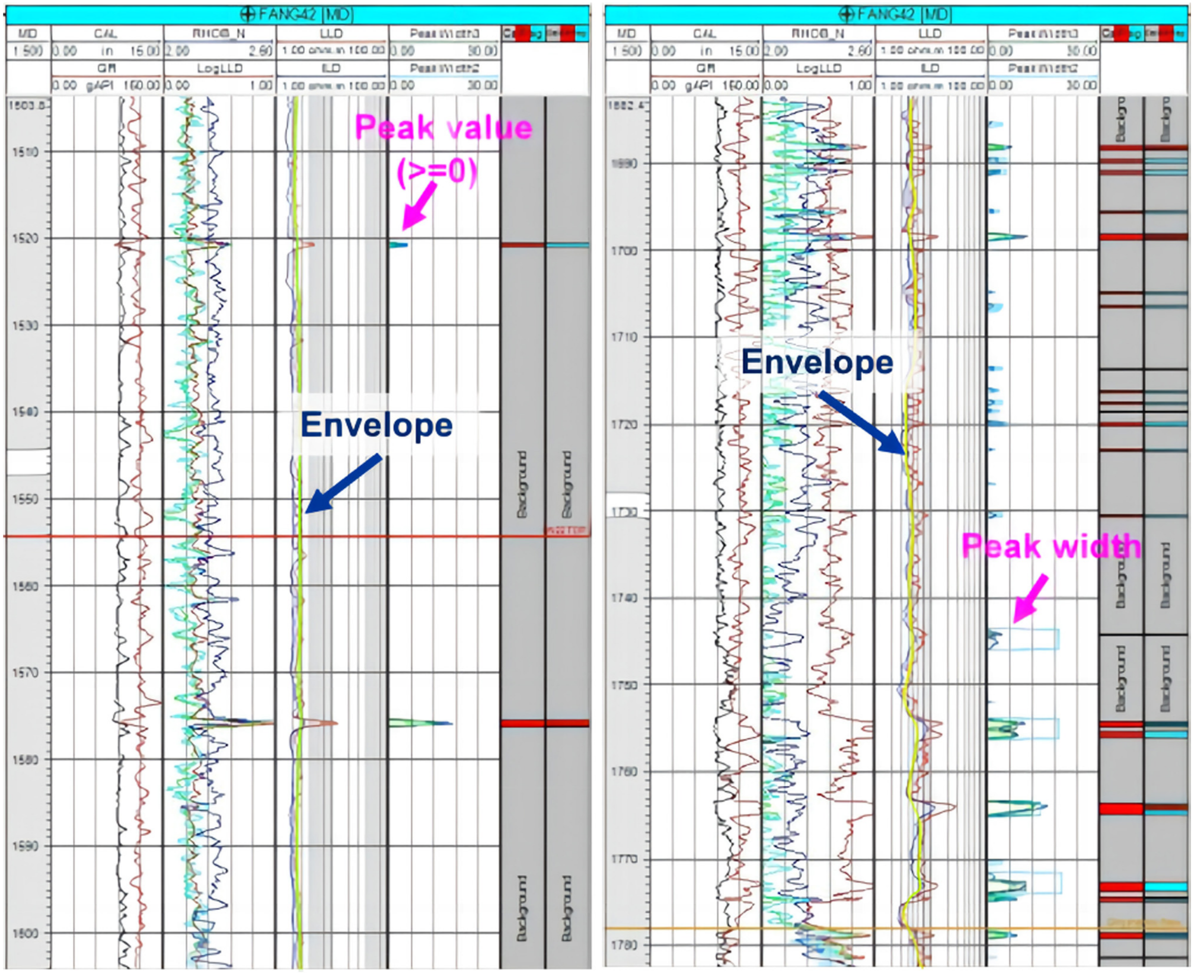

Figure 2. Identifying the envelope thin clip layer based on deep side-to-electrical resistivity curve.

for different levels of translation (for example, the distribution of deep lateral resistivity of the envelope translation, 0.04, 0.06, 0.02), the calculation of three different peak height and peak width, combined with core and cuttings logging data of the logging, using different translation quantity calculation and identify thin interlining, So as to achieve the best thin layer recognition effect. In practical applications, it is found that density logging has a good indication of the type of thin interlayers, and the thin interlayers are divided into calcareous interlayers (RHOB > 2.4 g/cc) and sandy interlayers with a logging density of 2.4 g/cc as the boundary (RHOB < 2.4 g/cc).

3.4. Calculation Ro with Ancient Paleo Buried Depth

In the Songliao Basin, a large number of Ro analysis tests had been carried out in the long-term oil and gas exploration and development process. This study was completed on the basis of 661 Ro data points from 163 wells. Generally speaking, there was a linear positive correlation between Ro and depth, and the slope of the relationship between Ro and depth in different wells was basically the same (Figure 3), but the intercepts were quite different (such as in the Gulong sag). The Qingshankou Formation in the Songliao Basin is dominated by shale, and other lithologies are mainly various sandstones, limestones, with similar thermal conductivity. After the Qingshankou Formation period, the structure of the entire Songliao Basin was stable, and there was no major uplifting and denudation during this period. It can be assumed that the geothermal gradient in the study area is consistent.

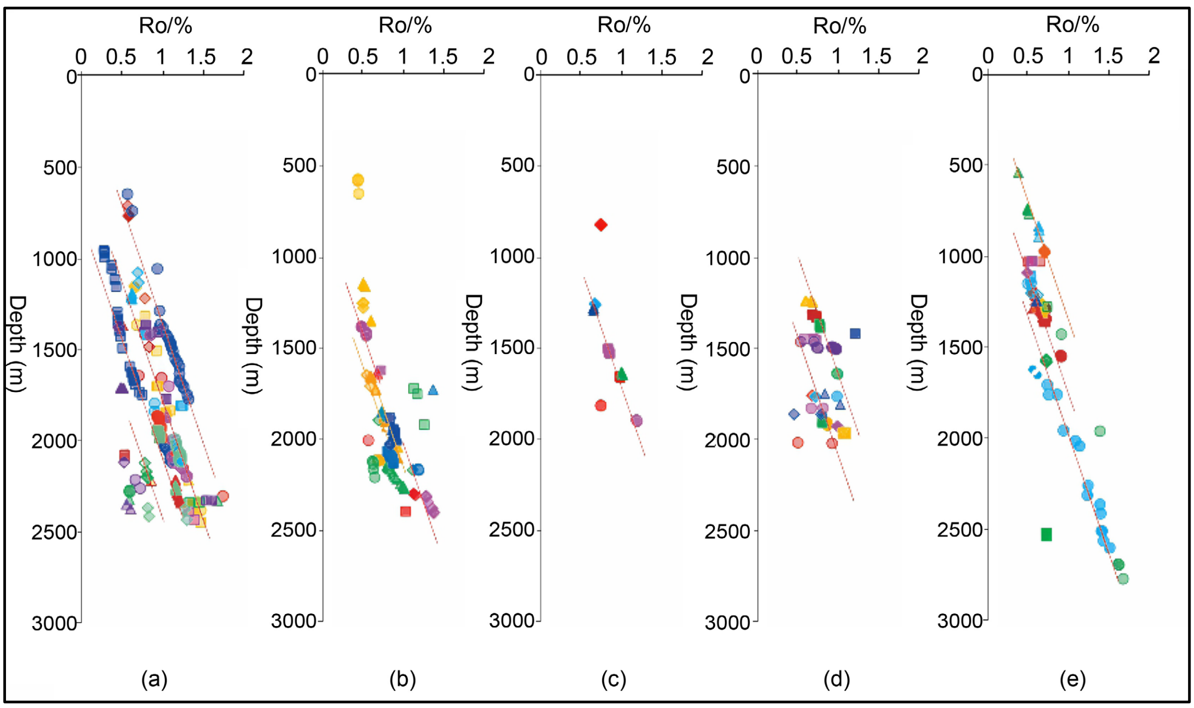

Figure 3. Varchange of vitrinite reflectance and reed exercise map in different tectonic units in Songliao: Gulong Sag (a), Qijia Sag (b), Chaoyanggou Terrace (c), Daqing Placanticline (d), Sanzhao Sag (e).

First, the slope of the linear relationship between Ro and buried depth is analyzed, and then the intercept of the linear relationship between Ro and buried depth in each well is evaluated based on the slope. Due to the large difference in the number of Ro data points in each well in the study area, when the number of data points in one well is less than 3, the uncertainty of the linear relationship based on data regression is large, and it is not suitable to participate in the evaluation of the slope of the linear relationship between Ro and buried depth in the whole Basin. Therefore, all data of 28 wells with more than 5 Ro data points were firstly used to establish the linear relationship between Ro and burial depth and determine the slope. Then, based on the slope, the intercept of the linear relationship between Ro and burial depth in each well was evaluated (**Figure 4**), which was closely related to Formation denudation and uplift, and could indirectly evaluate the ancient burial depth of the Formation.

At present, the research on thermal evolution degree mainly analyzed the well as a unit, established a plan, or studied the time evolution characteristics and spatial distribution characteristics of thermal evolution degree through Basin simulation, and rarely established a 3-D model of vitrinite reflectance based on actual measurement data. The Qingshankou Formation in the Songliao Basin had a wide distribution range, large stratum thickness, and large variation in burial depth, resulting in a large change in its Ro value in the study area. It was necessary to establish a 3D Ro model to analyze the spatial characteristics of Ro in detail. The 3-D model of Ro could be established by spatial interpolation method using the measured data of Ro as input. In addition, considering the linear

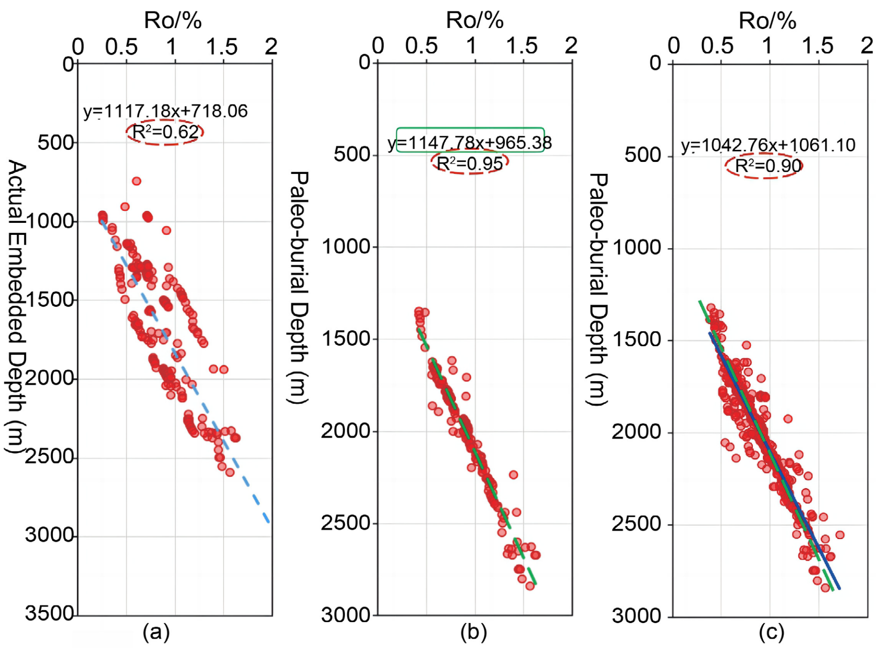

Figure 4. Wells with more than 5 groups of Ro data points in Songliao Basin: the intersection of Ro and actual embedded depth (a), the intersection of Ro and estimated paleo-burial depth (b); 163 wells in Songliao Basin with Ro and assessed paleo-burial depth deep intersection chart (c).

relationship between Ro and burial depth, the 3-D model of Ro could be established by directly using the formula to calculate the restored 3-D model of ancient burial depth. But both methods had flaws. The spatial difference method cannot effectively consider the relationship between Ro and burial depth, and the direct calculation of Ro model cannot effectively consider the measured data in the well. Therefore, in order to synthesize the measured data of Ro and a new method was designed to build the 3D model of Ro:

1) First, established the intercept plan according to the intercept of each well calculated from the relationship between Ro and burial depth;

2) Calculated the 3D burial depth model according to the elevation of the wellhead filling core and the 3D structural model;

3) Calculated the Ro value of each grid in the 3D structural model based on the intercept plan and the 3D buried depth model, as a trend model;

4) Taking the measured Ro data as the input data, and with the calculated Ro trend model as the constraint, established the Ro 3-D model.

This method not only fully considered the measured data of Ro in the well, but also considered the linear relationship between Ro and burial depth, and the modeling effect was the best.

3.5. Calculation TOC in the Study Area

There were many methods for TOC content prediction, but the ΔLogR method developed by Passey et al. (1990) is the most widely used. Therefore, in this study, the Passey method was used as the main body to predict the TOC content of Qingshankou Formation.

$$\Delta \mathrm{LogR} = \log\left(\mathrm{RESD}/\mathrm{RESDBase}\right) + c \times \left(\mathrm{PHILog} - \mathrm{LogBase}\right) \tag{1}$$

$$\mathrm{TOC} = a \times \left(\Delta \mathrm{LogR} \times 10^{0.297 - 0.1688\mathrm{LOM}}\right) + b \tag{2}$$

where, ILog was one of porosity logging acoustic time difference AC, DEN, RHOB, and NPHI; LogBase was the baseline corresponding to porosity logging; RESD was one of LLD or ILD; RESDBase was the deep resistivity logging baseline; a, b, c were constants. According to Passey method, the value of organic matter maturity (LOM) was determined based on Ro, and then TOC was determined based on ΔLogR.

The TOC value on a single well can be calculated through the above Equation (1) and Equation (2). Afterwards, it was necessary to extend the uphole data to the 3-D geological body with the help of geostatistical methods. The specific operation process was as follows. 1) Discretized TOC. In this process, the average method was used to reasonably distribute the TOC data to the discrete grids passing through the well; 2) Data analysis. Using the variation function analysis method, the exponential function was fitted into the variation function curve, and each parameter of the variation function is determined; 3) Interpolation algorithm. The Sequential Gaussian Simulation algorithm was used to build the 3-D TOC model.

3.6. Recognition Minerals Content Artificial Neutron Network

Although the Qingshankou Formation had a set of semi-deep lacustrine and deep lacustrine organic-rich shale sedimentary strata with wide distribution and relatively stable thickness distribution, the mineral content in the mud shale reservoir varies greatly in the horizontal and vertical directions. It was an important manifestation of the heterogeneity of shale reservoirs, which is crucial to the evaluation of sedimentary characteristics, fracturing properties, and reservoir physical properties. There were various types of minerals in shale reservoirs, and minerals are usually classified into 3 - 4 categories: siliceous/felsic minerals (including quartz, potassium feldspar, plagioclase), clay minerals (including various clay minerals and mica), carbonate minerals (including calcite, dolomite, siderite), and other minerals (including pyrite, barite). Through core testing, it was found that the mineral content was felsic, clay and carbonate minerals. In this paper, an artificial neural network was used to fit the core tested siliceous mineral content (quartz and feldspar) and clay mineral content (illite, chlorite, kaolinite, and mica). The specific prediction process was as follows: 1) Data preparation and grouping. In order to prevent overfitting, this paper divided the data into five groups for cross-checking, of which four groups are training samples and one group is testing samples. A total of five trainings were carried out. Thus, 5 neural networks are established; 2) Neural network training. BP neural network was used to build a neural network with logging data and siliceous and clay mineral content as output; 3) Result processing. In mineral content prediction, the average value of the five network results was taken as the final prediction result, so the prediction was more stable and accurate. The carbonate mineral content was determined from the predicted siliceous mineral content and clay mineral content.

The process of 3-D modeling of mineral content was the same as the modeling process of TOC content. It also performed well logging prediction mineral content assignment and variogram curve analysis, and then used Sequential Gaussian Simulation (SGS) algorithm to perform spatial difference, so as to establish silicon 3-D model of siliceous, clay, and carbonate mineral content.

3.7. Lithofacies Division and Identification

Shale can be subdivided into many subfaces, and different subfaces have different contributions to shale oil production. Subdivision of lithofacies provides an important geological basis for identifying high shale oil and gas production areas (Liu et al., 2020). The classification methods of shale lithofacies can be divided into three categories: one was to define mud shale lithofacies based on minerals, sedimentary characteristics, biological characteristics. The research is limited to the core scale, and it is difficult to expand to three-dimensional space, the other was to define lithofacies based on petrophysical properties, mechanical properties (Shu et al., 2021). This method was basically directly inherited from traditional lithofacies research, and its disadvantage was that the research is limited to the core scale, and it was difficult to expand to 3-D space; the third type was based on mineral composition and organic matter content. This method fully considered the control factors of shale gas sweet spots, and organically combines natural gas content and rock fractability. At the same time, the logging response was obvious and the logging prediction results were reliable and therefore more and more widely used.

In this paper, the lithofacies of Qingshankou Formation mud shale were mainly divided based on mineral content and TOC content. First, four lithofacies (Felsic shale, Clay shale, Calcareous shale, Mixed shale) were identified based on the siliceous mineral content, clay mineral content and carbonate mineral content of 50%. According to the standard of TOC content of 2% and 3% (TOC < 2% for low, 2% < TOC < 3% for medium TOC, TOC > 3% for high TOC), the lithofacies were further divided into 12 categories (Figure 5). In addition to mud shale of Qingshankou Formation in Songliao Basin also had a large number of calcareous and sandy interlayers. Therefore, a total of 14 lithofacies were identified in the Qingshankou Formation, including 12 shale lithofacies and 2 interlayer lithofacies.

The logging prediction methods of mud shale lithofacies can be divided into two categories. One was to use neural network pattern recognition technology to directly determine the type of shale lithofacies at each data point of the logging curve by using the logging curve or the characteristic parameters extracted from it as the input and the shale lithofacies as the output. Another type of method was an indirect method. The regression fitting technology of neural grid was used to predict the mineral content and TOC content of shale by taking logging curve or its extracted characteristic parameters as input and mudstone mineral content as output. Then, the shale lithofacies was determined according to the classification criteria of mineral content and TOC content. Both approaches had their own advantages. This paper adopted the second method for three main

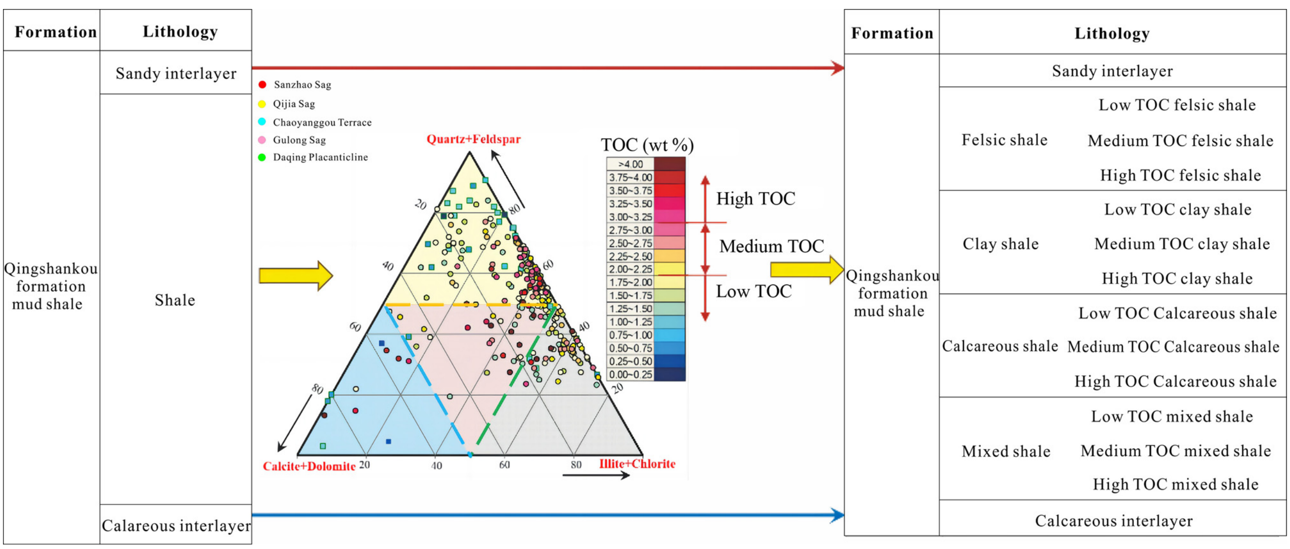

Figure 5. Lithofacies division method of Qingshankou formation mud shale in Songliao Basin.

reasons following. First of all, due to the limited XRD data points in the study area and the large amount of TOC content data, in order to make full use of various data, the second method was adopted, the second method was adopted, which was to predict the mineral content and TOC content respectively and then lithofacies was divided. Secondly, because there were many types of shale lithofacies to be identified, direct pattern recognition was less effective for predicting lithofacies, while the second method had a higher accuracy rate and better effect. Finally, the second method established the TOC model and the mineral model at the same time in the process of predicting lithofacies. On the one hand, these models had many other applications, and at the same time, the shale lithofacies can be re-divided according to different needs, which was more flexible. The specific steps were: The TOC content first was predicted by ΔLogR. Then the siliceous and clay mineral contents were predicted by using neural network with the input of multiple logging curves. The carbonate mineral content was calculated based on the predicted siliceous and clay mineral contents. Finally, the Qingshankou Formation was divided into 14 kinds of lithofacies according to the lithofacies classification standard shown in Figure 5.

4. Results

4.1. 3-D Model of Thin Interlayers

After identifying calcareous thin interbedded and sandy thin interbedded in a single well, Qingshankou Formation can be divided into three lithofacies, namely calcareous thin interbedded, sandy thin interbedded and mud shale. The reason for this division is that the thickness of calcareous and sandy interbeds is very large, far exceeding the shale lithofacies classification standard based on mineral type and TOC, which is not conducive to the later shale lithofacies division and modeling.

Figure 6 shows the distribution characteristics of thin interlayers in the horizontal and vertical directions. The thin interlayers are mainly distributed in the middle and lower parts of Qing 2 member and Qing 3 member and the upper part of Qing 1 member, while the calcareous interlayers are mainly distributed in the northern part of the study area. A small part is distributed in the west and south, with a maximum thickness of 80 meters, while sandy interlayers are mainly distributed in the northwest and south of the study area, with a maximum thickness of nearly 80 meters. At the same time, in order to better study the spatial distribution, according to Qing 1 member, Qing 2 member and Qing 3 member, the isopach maps of calcareous interlayers and sandy interlayers were calculated respectively. The calcareous interlayer has the largest thickness and the widest distribution in the Qing 1 member; its distribution in the Qing 2 member is the smallest, and is mainly confined to the northern part of the study area; and its distribution in the Qing 3 member is very similar to the Qing 1 member. Sandy interlayers are most widely distributed in Qing 1 member, mainly in the north and west of Gulong sag and the south of Sanzhao sag; The

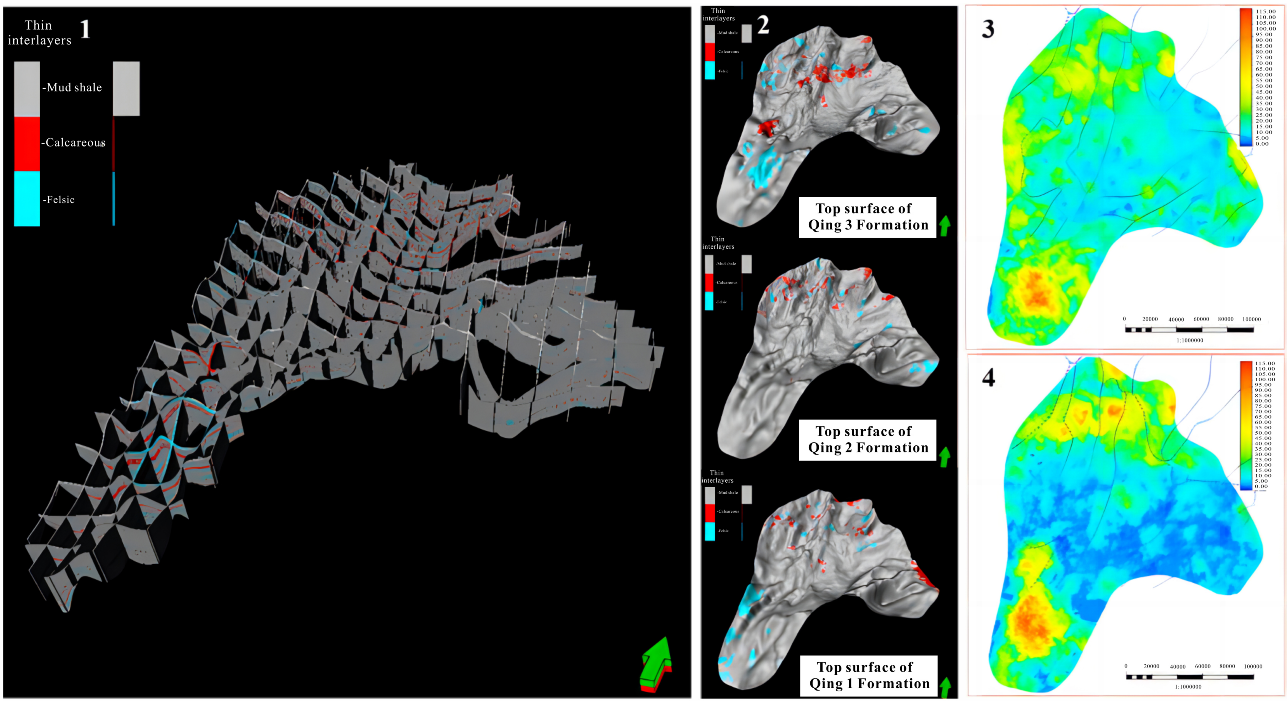

Figure 6. 1—A grid map of interlayer model; 2—A 3D model of a thin interlayer in Songliao Basin; 3—An isometric map of thin calcareous interlayer; 4—A thin sandy layer interlayer isometric diagram in Qingshankou Formation in Songliao Basin.

sandy interlayers of Qing 2 member are mainly distributed in the northern part of the Basin, mainly in the northern part of the Gulong sag; The sandy interlayers of Qing 3 member are mainly distributed in the northern and western parts of the Gulong sag.

4.2. 3-D Model of Ro

According to the 3D model of thermal maturity Ro of Qingshankou Formation in Songliao Basin (Figure 7), the Ro value of the Gulong sag is significantly higher than that of other parts of the study area, and the highest value appears in the central and southern part of the Gulong sag; although the Ro value of the Sanzhao sag is lower than that of the Gulong sag, its internal There are also local high values, mainly in the eastern part of the Sanzhao sag. The distribution law of Ro in Qing 1 member, Qing 2 member and Qing 3 member is basically the same, and it reaches the maximum value in the middle of the Gulong sag in the east of the study area, and the Gulong sag is significantly larger than other areas such as Sanzhao sag. In addition, local high values also appeared in the eastern part of the Sanzhao sag. This indicates that the thermal evolution degree of Gulong sag is higher. Although in the same basin, the differences in sedimentary environment and sedimentary burial depth in different tectonic units lead to different thermal evolution, and then lead to the difference in Ro.

4.3. 3-D Model of TOC

According to the 3-D geological model established, it is concluded that: on the

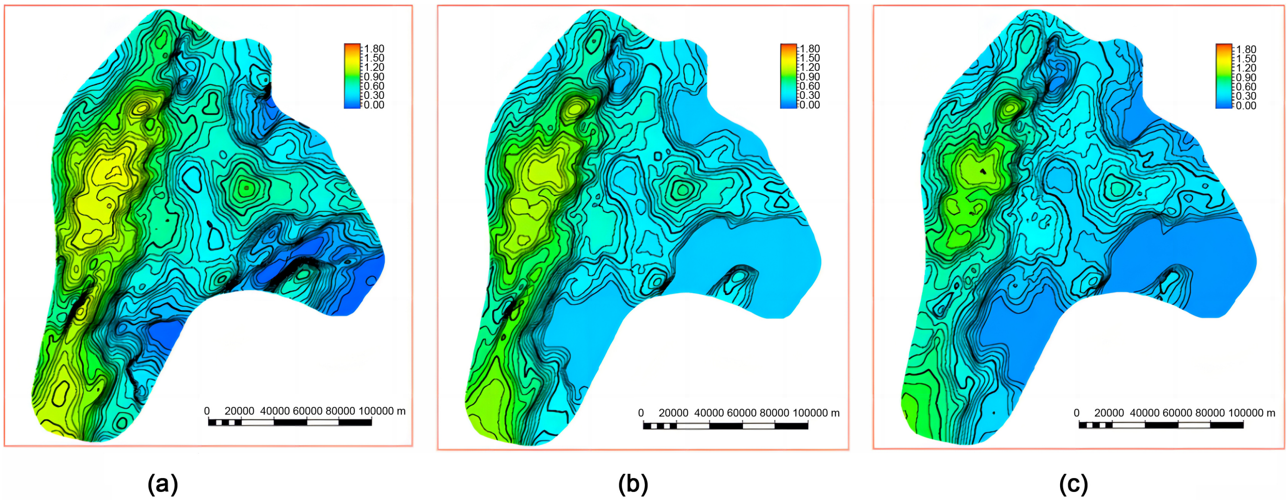

Figure 7. 1—A grid map of interlayer model; 2—A 3D model of a thin interlayer in Songliao Basin; 3—An isometric map of thin calcareous interlayer; 4—A thin sandy layer interlayer isometric diagram in Qingshankou Formation in Songliao Basin.

horizontal plane (Figure 8(b), Figure 8(d), Figure 8(f)), the high TOC content in Qing 1 member is mainly distributed in the middle part of Sanzhao sag, on the horizontal plane, while the TOC content in Gulong sag is relatively low. However, the high TOC in Qing 2 member is mainly distributed in Gulong sag, especially in the northern part of Gulong sag, while the TOC in Sanzhao sag is low. Vertically (Figure 9), TOC content in Qing 1 member is the highest, and gradually decreases from bottom to top. Similar to Qing 3 member, Qing 2 member is significantly smaller than Qing 1 member, and gradually smaller from bottom to top. In addition to analyzing the contour map of TOC content, this paper also analyzes the contour map of shale with different TOC content. As shown in Figure 10, according to the isopach map of shale with TOC > 3%, high TOC shale mainly occurs in the southeast and east of the Basin, with a maximum thickness of only 90 meters; while the shale with TOC between 2% and 3% mainly occurs in Northwest of the study area. There are also local high values in the northwest and southeast of the Basin. The average thickness of the entire Basin is about 100 m, which is significantly larger than the shale with TOC > 3%. According to the stratified statistical analysis (Figure 10), the shale with TOC content greater than 2% is mainly distributed in the Qing 1 member, and Qing 2 member and Qing 3 member are very few.

The reason for the uneven distribution of regional TOC is due to differences in sedimentary environments. The Cretaceous transgression event provided favorable conditions for the formation of black shale in Songliao Basin, especially the high TOC black shale in Sanzhao Chaoyang Valley area (Wang et al., 2022). The heterogeneity of TOC in different layers in the vertical direction is mainly due to differences in material sources. The Cretaceous transgression event mainly occurred in the sedimentary period of Qing-1 Member. The transgression brought abundant organic matter, and caused salinity differences, resulting in water stratification, which is conducive to the preservation of organic matter.

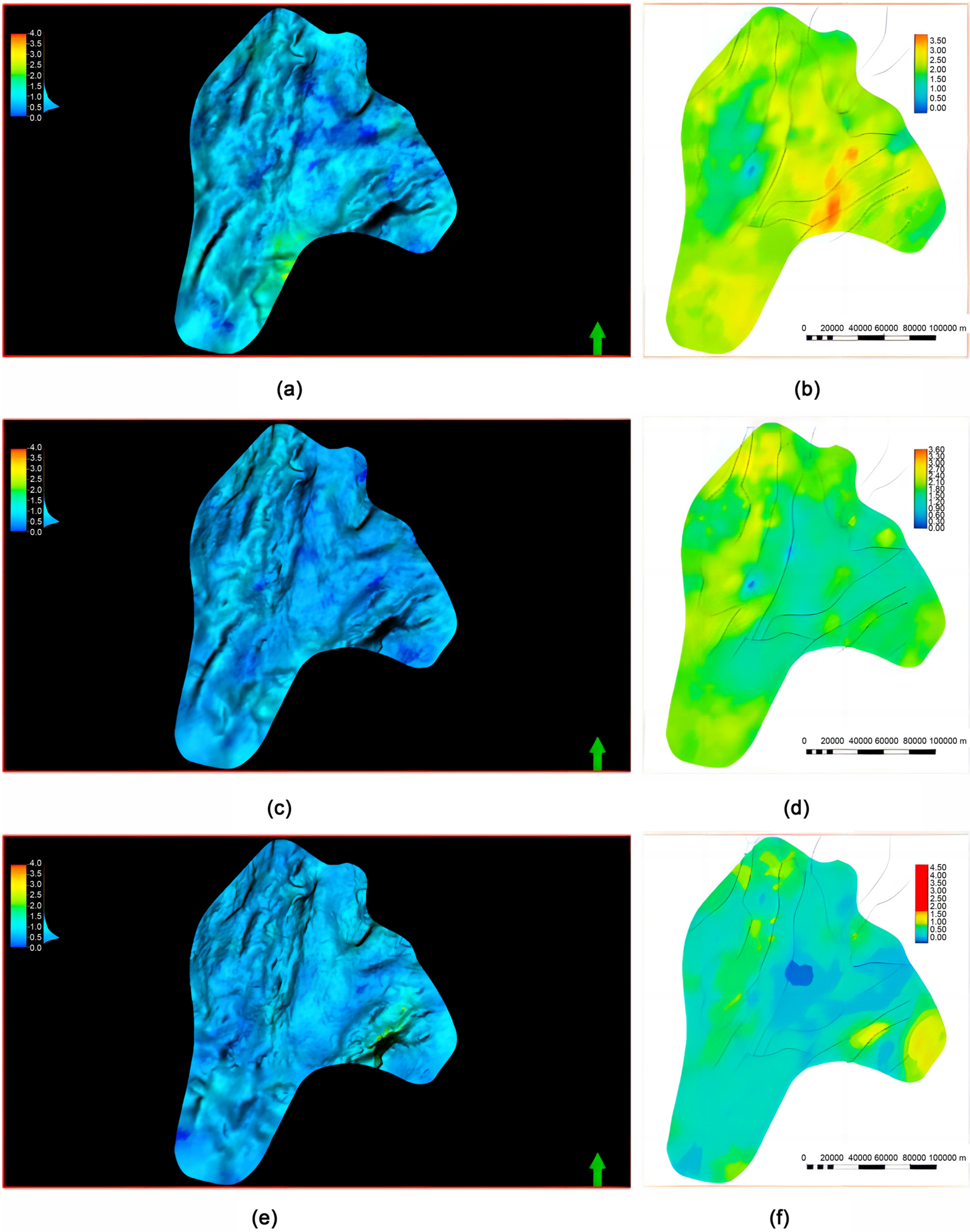

Figure 8. 3D model of TOC content in Songliao Basin: the surface of the Qing 1 member, the Qing 2 member, and the Qing 3 member ((a), (c), (e)); the average contour map of segment TOC content of the Qing 1 member, the Qing 2 member, and the Qing 3 member ((b), (d), (f)).

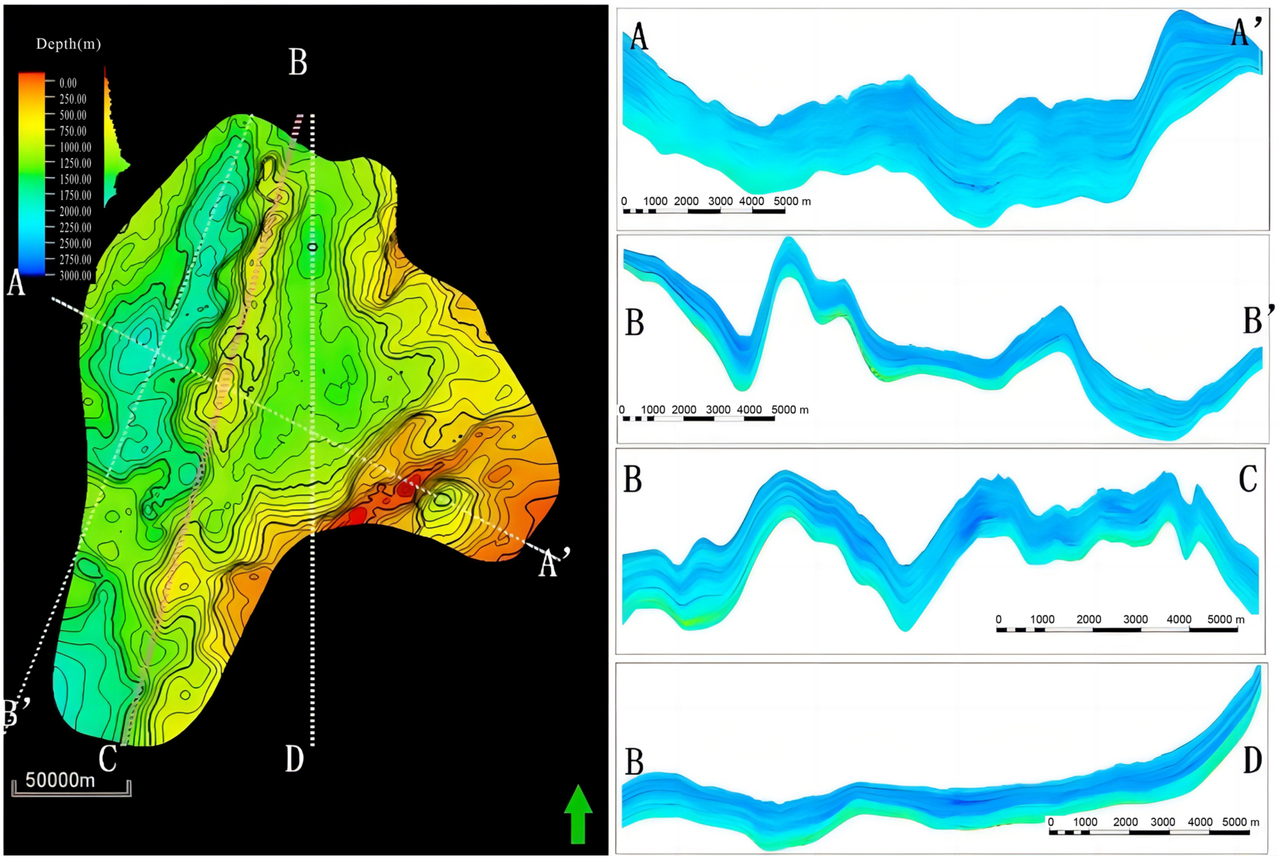

Figure 9. Profiles in four directions of the TOC content model of the Qingshankou formation in the Songliao Basin.

4.4. 3-D Model of Minerals

Figure 11 showed the 3-D property model of the content of siliceous minerals. It can be seen that the average content of siliceous minerals is mainly between 30% and 70%. According to the profile and plane contour map (**Figure 11(b)**), siliceous minerals of Qingshankou Formation were mainly developed in the Qing 2 and Qing 3 member vertically, and mainly distributed in the northwest and west of the Basin horizontally. Among Qing 3 member, the Qing 1 member has the lowest siliceous mineral content, the Qing 3 member has the highest content, and the Qing 2 member has the middle content.

The 3D model of clay mineral content is shown in **Figure 12**. The average content of clay minerals is mainly between 30% and 70%. From the clay mineral content profile (right panel in **Figure 12**), it can be seen that clay minerals are mainly developed in the Qing 1 member in the northern part of the Basin, while the Qing 1 member is mainly developed in the southern part of the Basin, and the Qing 2 and Qing 3 member are also relatively developed. From the flat contour map of clay minerals, the content of clay minerals is relatively high in the southwest and east of the Basin, with an average content of about 40%. Among the three strata of Qingshankou Formation, the Qing 1 member has the highest clay mineral content, and its high value is mainly distributed in the Gulong sag and the eastern part of the Basin; the Qing 2 member has the middle content,

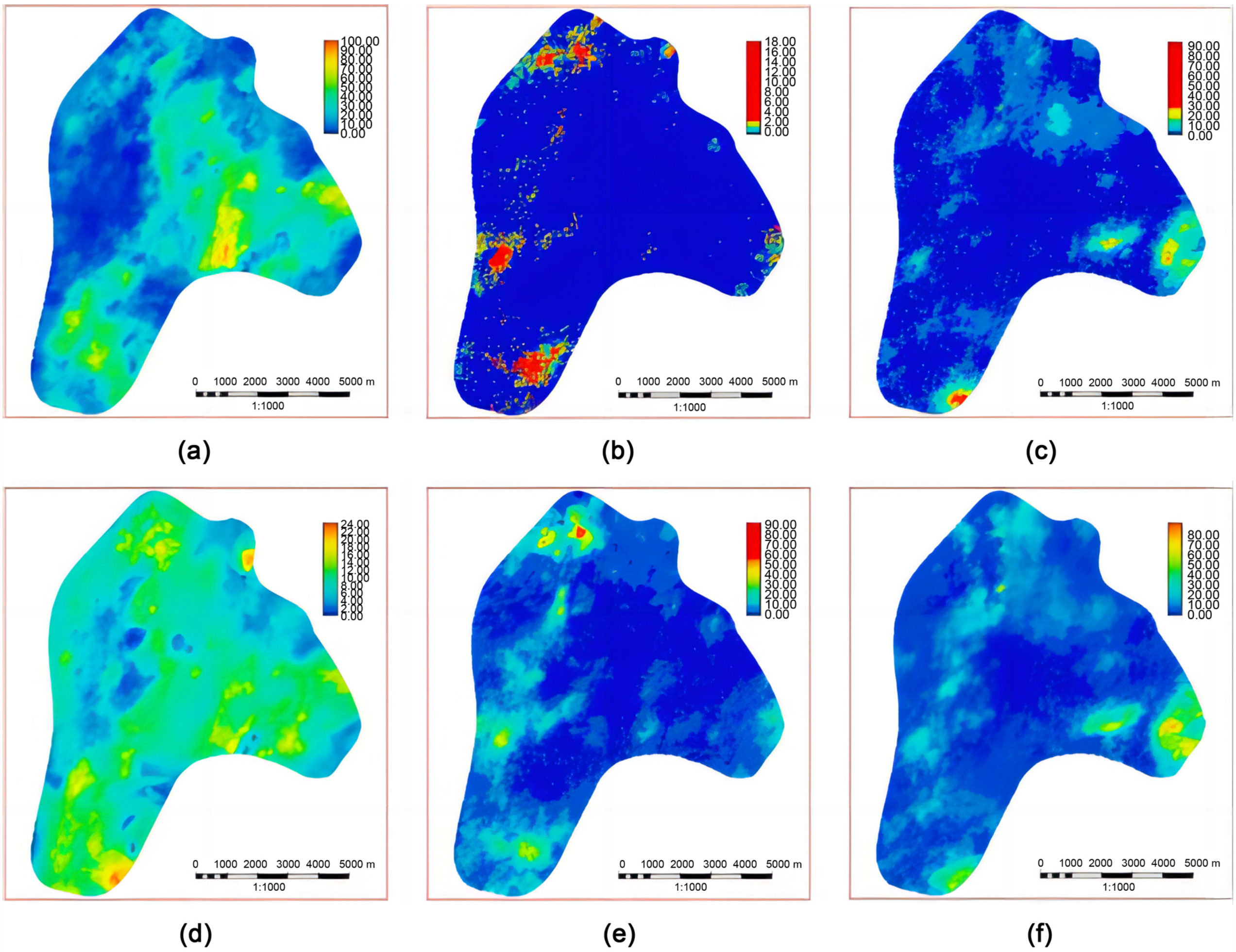

Figure 10. Isopach map of Qingshankou Formation shale in Songliao Basin: ((a), (b), (c)) are the top surfaces of Qing 1, Qing 2 and Qing 3 members with TOC content greater than 3% in order, ((d), (e), (f)) are in order the top surfaces of Qing 1, Qing 2 and Qing 3 with TOC content between 2% and 3%.

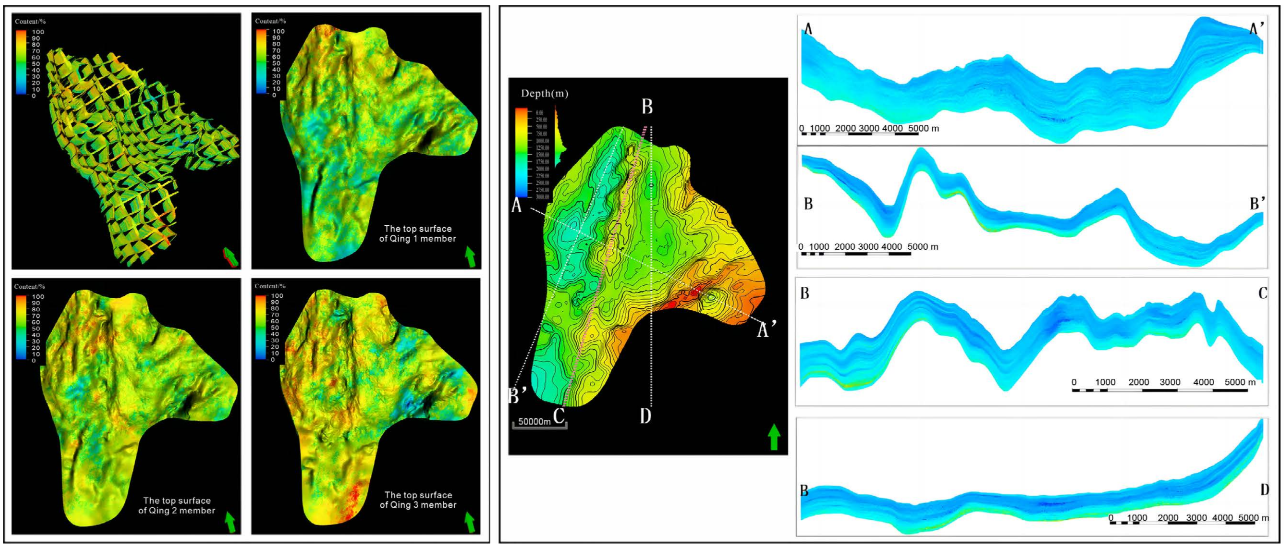

Figure 11. Model of siliceous mineral content of Qingshankou Formation—palisade map and layer map (left); four-way cross-section map of the Songliao Basin (right).

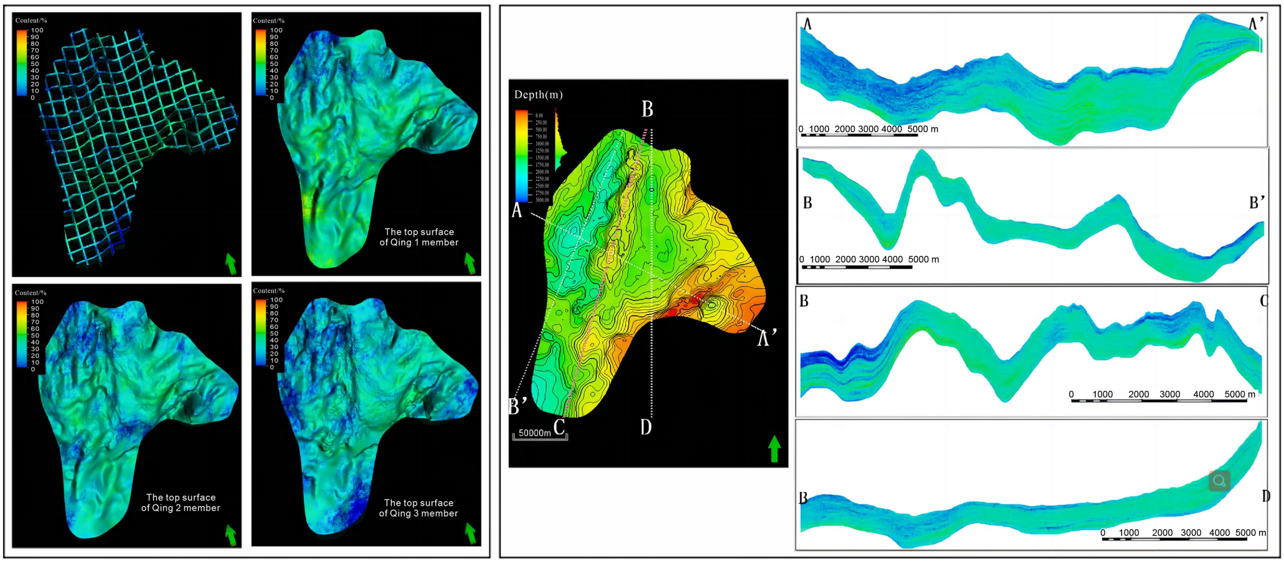

Figure 12. Model of clay mineral content of Qingshankou Formation—palisade map and layer map (left); right is the four-way section of the Basin (right).

and its high value is mainly distributed in the southern part of the Gulong sag and the Sanzhao sag in the south, the Qing 3 member has a similar distribution pattern to the Qing 2 member, but the content is slightly lower.

During the Qingshankou Formation, the east and southwest were the main sedimentary centers of the basin, so the content of clay minerals is relatively high in the southwest and east of the Basin. Moreover, due to the difference between the sedimentary environment and the input of the parent material, the difference of mineral components occurs, and the mineral content of clay in Sanzhao Sag is higher than that in Gulong Sag.

The 3D model of carbonate mineral content, as shown in Figure 13, is generally lower than that of siliceous mineral content and clay mineral content, with multiple local high values, including the northwest, northeast, southwest and south of the Basin. From the carbonate mineral content profile and plane contour map (the right image of Figure 13), it can be seen that among the three layers of the Qingshankou Formation, the Qing 1 member has the highest carbonate mineral content, and the high values are mainly distributed in the south of the Basin and the middle part of the Gulong sag; Qing 2 member is similar to Qing 3 member, and the high values are mainly distributed in the northwest and south of the Basin. The transgression mainly occurred during the qing 1 deposition period, which brought a large amount of marine matter, and chemical precipitation occurred in the basin and produced many carbonates, which led to the phenomenon that the mineral content of Qing 1 carbonate was generally higher than that of Qing 2 and 3.

4.5. 3-D Model of Lithofacies

Based on the established 3D model of TOC content, siliceous minerals, clay minerals and carbonate minerals, the 3D model of mud shale lithofacies in

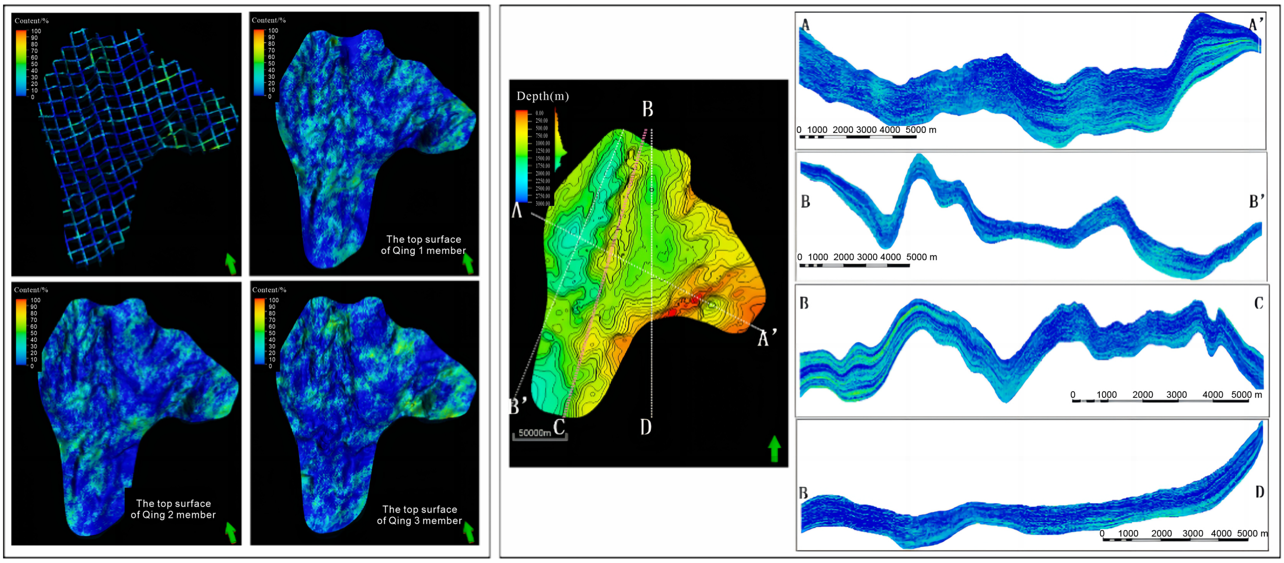

Figure 13. Carbonate mineral content model of Qingshankou Formation—palisade map and layer map (left); four-way profile of the Basin (right).

Qingshankou Formation of Songliao Basin was directly calculated and determined based on the criteria of mud shale lithofacies division in Figure 5 (Figure 14).

Due to the numerous types of lithofacies, the spatial distribution of shale facies in the Qingshankou Formation is mainly analyzed through the plane isopach map of lithofacies. Firstly, a lithofacial thickness map is established by taking the Qingshankou Formation as a whole. The Qingshankou Formation mud shale lithofacies are mainly low-TOC felsic shale, with a maximum thickness of more than 400 meters and an average thickness of about 300 meters; at the same time, low-TOC mixed shale is also developed, with a maximum thickness of more than 400 meters , but mainly concentrated in the central and southern part of the Gulong sag; in addition, middle TOC felsic shale and middle TOC mixed shale are also relatively developed; high TOC mixed shale and high TOC felsic shale are mainly found in the Sanzhao sag and The eastern part of the Basin is developed; other shale lithofacies are relatively undeveloped, and are locally distributed in the Basin. For example, high-TOC calcareous shale is mainly distributed in the interior of the Sanzhao sag, and mainly in the south of the Sanzhao sag, while high-TOC clay shale is mainly distributed in the east of the Basin.

By longitudinal comparison of lithofacies distribution characteristics of various shale in The Qing 1, 2 and 3 members of Qingshankou Formation (Figures 15-17), it can be seen that the lithofacies characteristics of shale in the Qing 1 member are very similar to that of the whole Qingshankou Formation, mainly characterized by low TOC felsic shale and mixed shale with a wider distribution range of low TOC felsic shale. Low TOC mixed shale is mainly distributed in the middle and south of Gulong sag, followed by medium TOC felsic shale and medium TOC mixed shale. High TOC felsic shale and high TOC mixed shale are mainly distributed in the Sanzhao sag and the eastern part of the Basin. Other

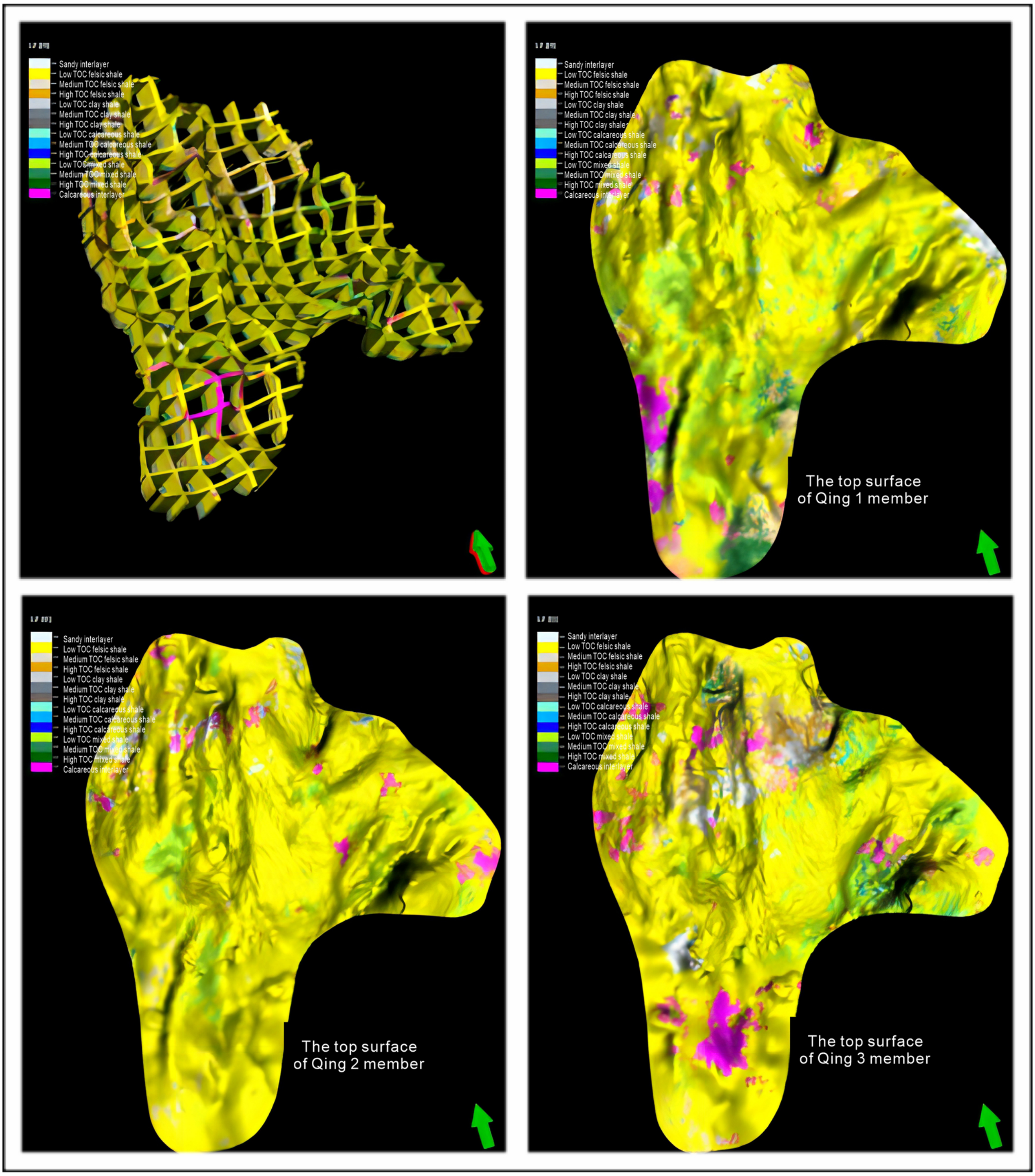

Figure 14. Lithofacies grid map and layer map of Qingshankou formation shale and the lithographic plane model diagram of the three sections of the Qingshankou Formation.

shale lithofacies are not developed and mainly occur locally in the Basin (Figure 15). The lithofacies of the Qing 2 member and 3 member are relatively simple, with low TOC felsic shale mainly developed, followed by low TOC mixed shale. Low TOC calc shale and medium TOC felsic shale are locally developed, while

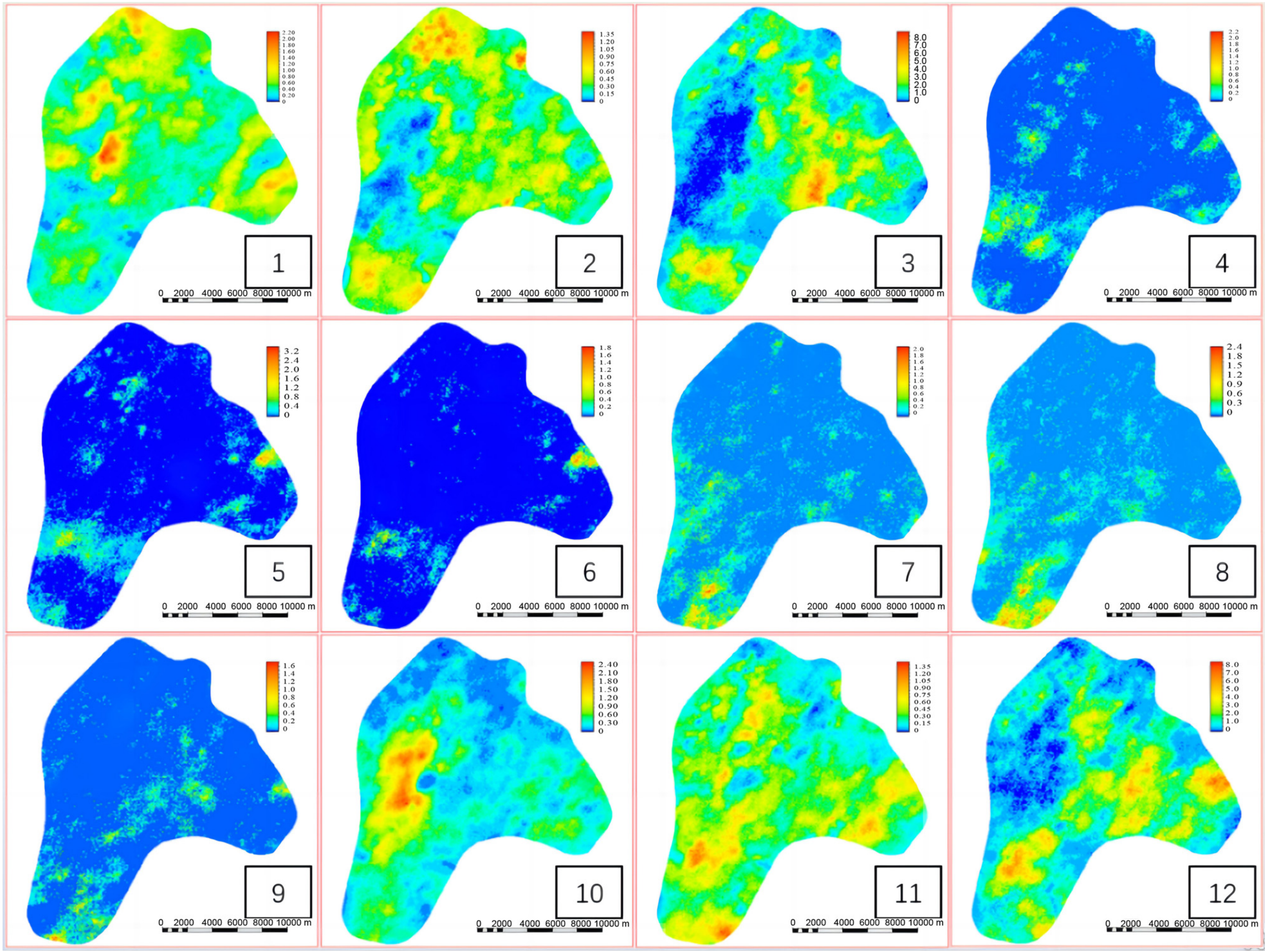

Figure 15. Net map of mud shale in Qing 1 member Formation in Songliao Basin: (1) low TOC felsic shale; (2) medium TOC felsic shale; (3) high TOC felsic shale; (4) Low TOC clay shale; (5) medium TOC clay shale; (6) high TOC clay shale; (7) low TOC calcareous shale; (8) medium TOC calcareous shale; (9) high TOC calcareous shale; (10) low TOC mixed shale; (11) medium TOC mixed shale; (12) high TOC mixed shale.

other shale lithofacies are distributed sporadically (Figure 16 and Figure 17).

In this paper, shale oil rich areas are identified based on the control effect of organic matter content and thermal maturity on original hydrocarbon generation. Hydraulic fracturing, the second factor affecting shale oil development, is affected by a variety of geological factors and engineering construction, which needs to be considered comprehensively. In terms of reservoir geology, mineral composition, interlayer and natural fracture have significant influence on fracturing, especially brittle mineral is an important content of shale reservoir evaluation. This paper mainly considers the influence of mineral composition on the mechanical properties of shale rock, analyzes its influence on the effect of hydraulic fracturing reservoir reconstruction, so as to identify the favorable area of shale oil. According to TOC content, brittle minerals and shale lithofacies distribution characteristics, compared with the upper part of Qing 1 member, Qing 2 member and Qing 3 member, the lower part of Qing 1 member has higher TOC content, slightly higher brittle minerals content, and the shale lithofacies is

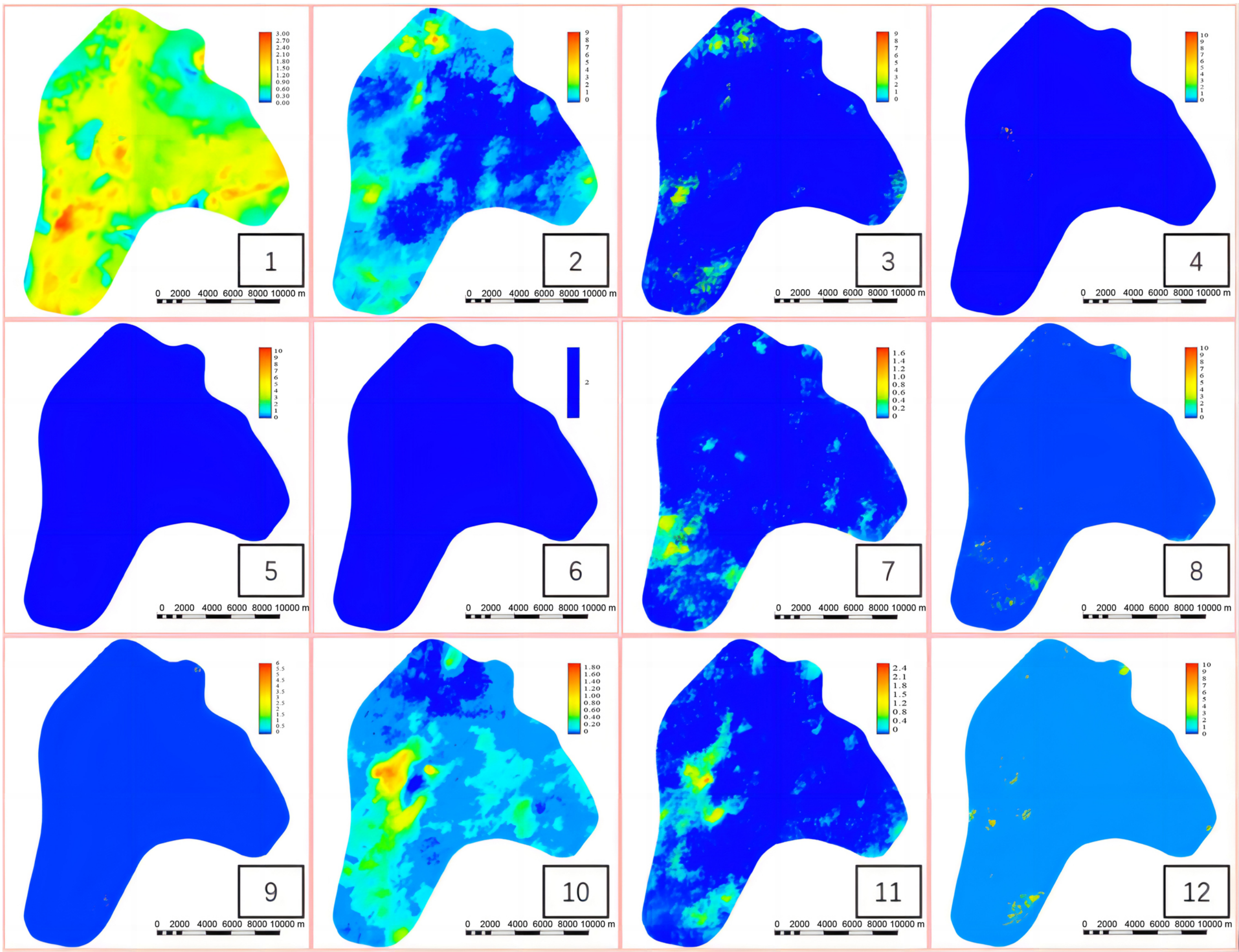

Figure 16. Net map of mud shale in Qing 2 member Formation in Songliao Basin: (1) low TOC felsic shale; (2) medium TOC felsic shale; (3) high TOC felsic shale; (4) low TOC clay shale; (5) medium TOC clay shale; (6) high TOC clay shale; (7) low TOC calcareous shale; (8) medium TOC calcareous shale; (9) high TOC calcareous shale; (10) low TOC mixed shale; (11) medium TOC mixed shale; (12) high TOC mixed shale.

dominated by middle-high TOC mixed lithofacies, which is more favorable to shale oil development and is a high-yield shale oil Formation in vertical direction.

TOC content, brittle mineral content and thermal evolution degree are mainly considered in the favorable shale oil areas in the Qing 1 member. In this paper, two high shale oil producing areas are identified in the Qing 1 member based on the isoline map of mud shale lithofacies, Ro and clay content (**Figure 18**). The first is the eastern part of Sanzhao sag (red dotted line), where the high TOC felsic shale and high TOC mixed shale have large thickness. Meanwhile, the thickness of medium TOC felsic shale and medium TOC mixed shale indicates that TOC content and brittle mineral content are relatively high in this sag. At the same time, although the degree of thermal evolution is slightly lower than Gulong sag, However, it is relatively high locally (about 0.8% - 1%), which is the best favorable area for shale oil development in Qing 1 member. The other is the

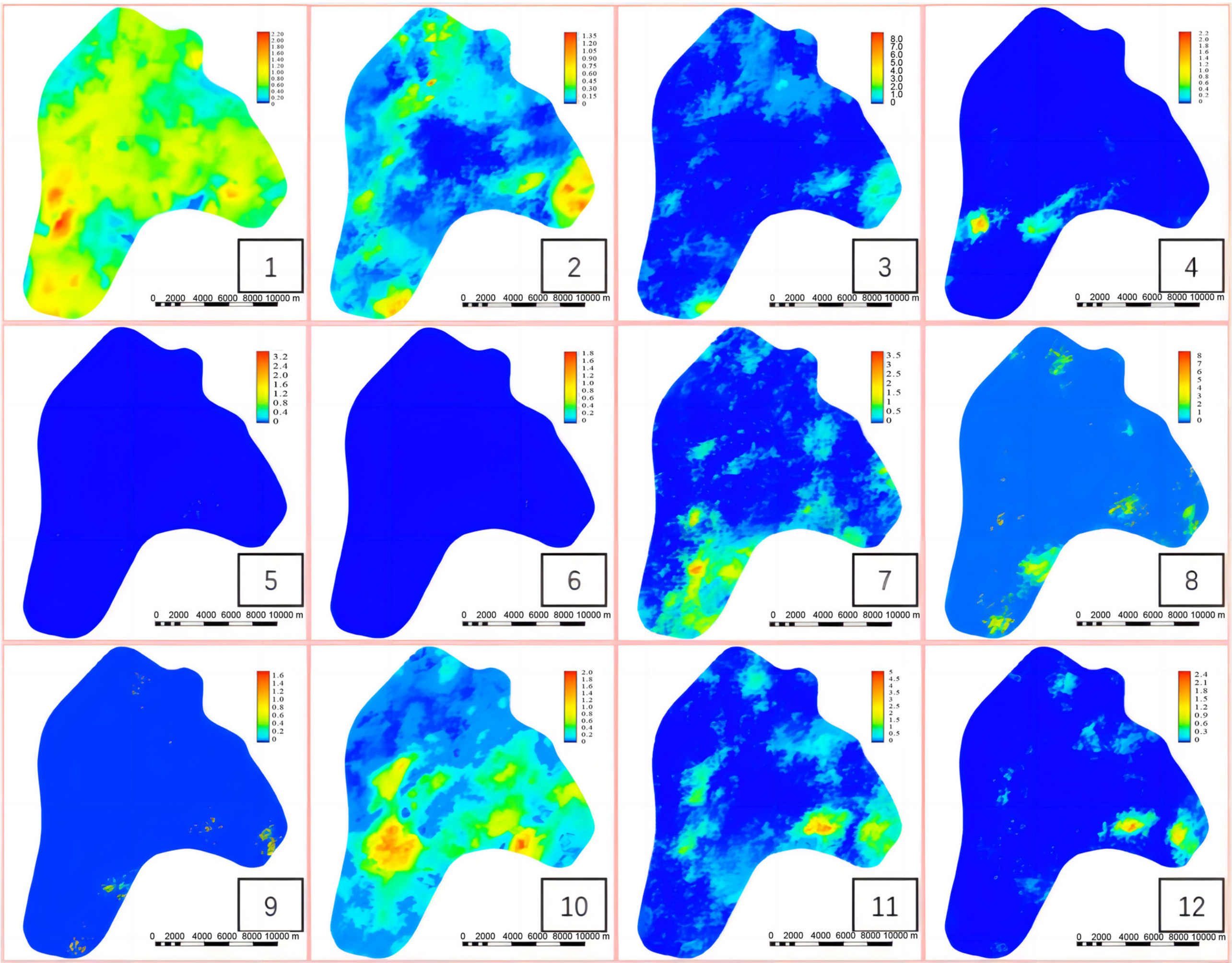

Figure 17. Net map of mud shale in Qing 3 member Formation in Songliao Basin: (1) low TOC felsic shale; (2) medium TOC felsic shale; (3) high TOC felsic shale; (4) low TOC clay shale; (5) medium TOC clay shale; (6) high TOC clay shale; (7) low TOC calcareous shale; (8) medium TOC calcareous shale; (9) high TOC calcareous shale; (10) low TOC mixed shale; (11) medium TOC mixed shale; (12) high TOC mixed shale.

northern Gulong sag (purple dotted line), where the TOC mixed shale thickness is relatively increased, and the TOC of the high TOC felsic shale and high TOC mixed shale thickness is relatively high, but the thickness of the high TOC felsic shale and high TOC mixed shale is lower than that of the eastern Part of the Sanzhao sag, and the thermal evolution degree is about 1.2%, which is significantly higher than that of the Sanzhao sag. Therefore, it is the second favorable area for shale oil development.

According to the three-dimensional modeling and spatial distribution law analysis of minerals, organic matter content, thermal evolution degree, thin interlayers, and shale rocks in this paper, the main characteristics of Qingshankou Formation shale oil reservoirs include: 1) Qingshankou Formation TOC The Qingshankou Formation has the highest content in the Qing 1 member, which is the main oil source layer in this area and an important target layer for shale oil development; 2) The Qingshankou Formation minerals are mainly quartz and

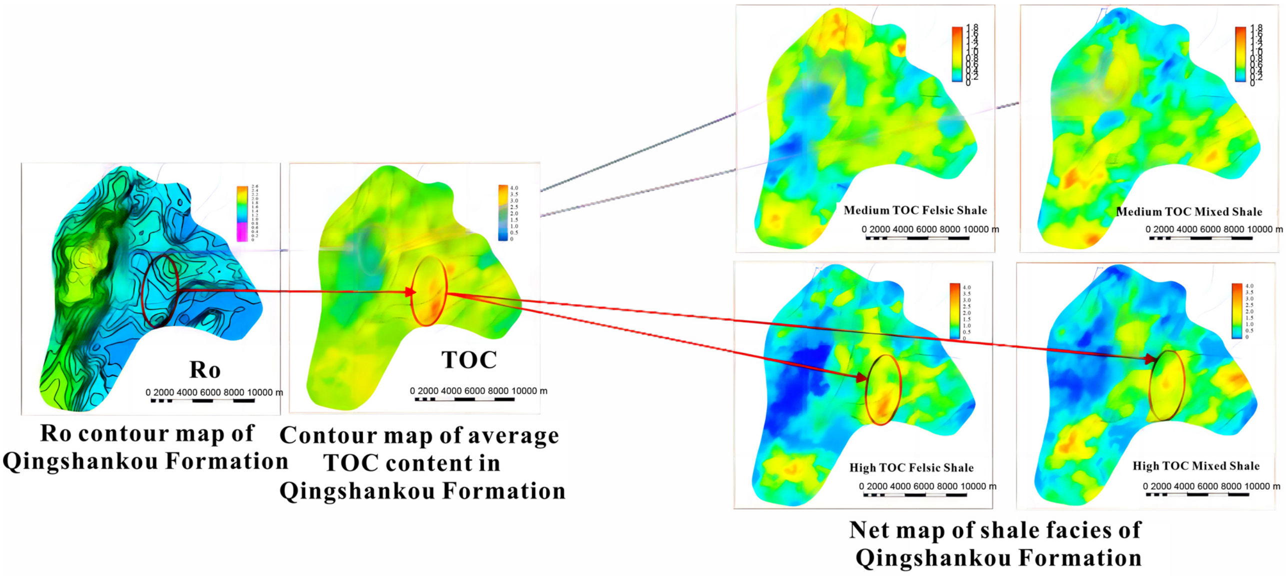

Figure 18. Plane prediction of shale oil sweet spots in Qingshankou Formation, Songliao Basin.

feldspar, and clay minerals and carbonate minerals are also relatively developed; 3) A large number of calcareous interlayers and sandy interlayers are developed in the Qingshankou Formation, especially in the northwest of the Basin, and its impact on shale oil development deserves attention; 4) The thermal maturity of the Qingshankou Formation is mainly distributed in between 0.5% and 1.5%, the maturity of the Gulong sag is higher, mainly between 1% and 1.5%, which is more favorable for shale oil development, while the maturity of the Sanzhao sag is lower, mainly at 0.5% to 1.2%.

5. Discussion

Shale oil is a self-generated and self-stored low permeability reservoir; its development is controlled by two main factors: one is shale oil reserves; the other is hydraulic fracturing effect (Jiang et al., 2016). Shale oil reservoirs are both source rocks and reservoirs, and their reserves are controlled by the original oil generation of organic matter, the short distance migration and the long distance migration (Zeidouni, 2023). The long-distance migration is controlled by migration channels and underground pressure systems, while the short-distance migration is mainly related to the development characteristics of adjacent strata or interlayers of organic-rich shale. Calcareous interbeds and sandy interbeds are extremely developed in Qingshankou Formation of Songliao Basin. In the process of hydrocarbon generation and pressurization of organic-rich shale, shale oil migrates to calcareous and sandy intercalation in different degrees under the combined action of pressure differential drive and diffusion. At the same time, calcareous interlayer and sandy interlayer are dissolved under the combined action of organic acid and hydrocarbon generation pressurization, and a large number of micro-fractures are formed. Therefore, calcareous intercalation and sandy intercalation may be favorable or unfavorable to shale oil development, which mainly depends on the joint influence of shale oil content, pore and fracture system development and thickness of thin intercalation. Based on the analysis and test results of thin section, fluorescence and porosity in Qingshankou Formation, Songliao Basin, and thin interlayer can promote the development of shale oil to a certain extent, but the influence of thin interlayer on hydraulic fracturing should be carefully treated. In addition, the contribution of thin interbeds to shale oil development requires a large number of production data for statistical analysis and verification.

1) LLD logs were used well to identify calcareous and sandy intersections with thin intersections, but there were inaccuracies when using DEN logs.

2) Calcareous and sandy interbeds identified by thin interbeds are removed as two separate lithofacies in the lithofacies division process, but as shale lithofacies continues to be classified, the subclasses also have calcareous and sandy minerals. Whether calcareous and sandy interbeds should be added to the Shale classification is questionable.

6. Conclusion

The envelope algorithm is effective in identifying thin interlayer, and the accuracy of LLD logging data is high;

The method of restoring paleo buried depth can expand basic modeling data and has good applicability;

ANN identifies lithofacies accurately.

Acknowledgements

1) Science and technology project of PetroChina exploration and production company "enrichment mechanism and sweet zone of tight oil/shale oil in the Songliao Basin". Approval number: 2021-06-01.

2) Research project of PetroChina Co., Ltd. "Research on shale oil enrichment law, resource potential and target evaluation of favorable zones". Approval number: 2021DJ1801.

3) Science and technology project of research institute of petroleum exploration & development "organic matter deFormation and its impact on organic matter pore development".

Conflicts of Interest

The authors declare no conflicts of interest regarding the publication of this paper.

References

Allix, P., Bumham, A., Fowler, T., Herron, M., & Symington, B. J. O. R. (2010). Coaxing Oil from Shale. *Oilfield Review, 22,* 4-15.

Cui, B. W., Chen, C. R., Lin, X. D., Zhao, Y., Cheng, X. Y., Zhang, Y. P., & Lu, G. Q. (2020) Characteristics and Distribution of Sweet Spots in Gulong Shale Oil Reserviors of Songliao Basin. *Petroleum Geology & Oilfield Development in Daqing, 39,* 11.

Holditch, S. A. (2013). Unconventional Oil and Gas Resource Development—Let's Do It Right. *Journal of Unconventional Oil and Gas Resources, 1-2,* 2-8. https://doi.org/10.1016/j.juogr.2013.05.001

Huang, Z. K., Chen, J. P., Xue, H. T., Wang, Y. J., Wang, M., & Deng, C. P. (2013) Microstructural Characteristics of the Cretaceous Qingshankou Formation Shale, Songliao Basin. *Petroleum Exploration and Development, 40,* 61-68. https://doi.org/10.1016/S1876-3804(13)60006-3

Jiang, Z. X., Zhang, W. Z., Liang, C., Wang, Y. S., Liu, H. M., & Chen, X. (2016). Basic Characteristics and Evaluation of Shale Oil Reservoirs. *Petroleum Research, 1,* 149-163. https://doi.org/10.1016/S2096-2495(17)30039-X

Liu, B., Sun, J. H., Zhang, Y. Q., He, J. L., Fu, X. F., Yang, L., Xing, J. L., & Zhao, X. Q. (2021). Reservoir Space and Enrichment Model of Shale Oil in the First Member of Cretaceous Qingshankou Formation in the Changling Sag, Southern Songliao Basin, NE China. *Petroleum Exploration and Development, 48,* 608-624. https://doi.org/10.1016/S1876-3804(21)60049-6

Liu, Z., Liu, G., Hu, Z., Dongjun, F., Zhu, T., Bian, R., Jiang, T., & Jin, Z. (2020). Lithofacies Types and Assemblage Features of Continental Shale Strata and Their Implications for Shale Gas Exploration: A Case Study of the Middle and Lower Jurassic Strata in the Sichuan Basin. *Natural Gas Industry B, 7,* 358-369. https://doi.org/10.1016/j.ngib.2019.12.004

Passey, Q. R., Creaney, S., Kulla, J. B., Moretti, F. J., & Stroud, J. (1990). A Practical Model for Organic Richness from Porosity and Resistivity Logs. *AAPG Bulletin, 74,* 1777-1794. https://doi.org/10.1306/0C9B25C9-1710-11D7-8645000102C1865D

Ryder, R. T., Jin, Q., McCabe, P. J., Nuccio, V. F., & Persits, F. (2003). *Qingshankou-Putaohua/Shaertu and Jurassic Coal-Denglouku/Nongan Total Petroleum Systems in the Songliao Basin, China*. U.S. Geological Survey Bulletin 2203-A.

Shang, F., Zhou, H. Y., Liu, Y., Zhou, X. X., Wang, L., Bi, H., Wang, G. C., Song, L., & Chen, R. Q. (2022). A Discussion on the Organic Matter Enrichment Model of the Nenjiang Formation, Songliao Basin: A Case Study of Oil Shale in the 1st and 2nd Members of the Nenjiang Formation. *Geology in China, 47,* 236-248.

Shu, Y., Bao, H., Zheng, Y., Chen, M., Lu, Y., Liu, H., Peng, W., Zhou, L., Ma, Y., Wen, Y., Wang, Q., & Zhang, Z. (2021). Lithofacies Types, Assemblage Characteristics, and Sedimentary Evolution Model of Lacustrine Shale in Dongyuemiao Formation of Fuxing Area. *Frontiers in Earth Science, 9,* Article ID: 772581. https://doi.org/10.3389/feart.2021.772581

Tian, Z. Y., Han, P., & Xu, K. D. (1992). The Mesozoic-Cenozoic East China Rift System. *Tectonophysics, 208,* 341-363. https://doi.org/10.1016/0040-1951(92)90354-9

Tourtelot, H. A. (1964). Minor-Element Composition and Organic Carbon Content of Marine and Nonmarine Shales of Late Cretaceous Age in the Western Interior of the United States. *Geochimica et Cosmochimica Acta, 28,* 1579-1604. https://doi.org/10.1016/0016-7037(64)90008-0

Wang, L., Zhou, H. Y., Shang, F., & Zhou, X. X. (2022). Element Geochemical Characteristics of Black Shale and Paleo-Sedimentary Environment Restoration the Cretaceous in the Northern Songliao Basin. *Chinese Journal of Geology, 57,* 156-171.

Zeidouni, M. (2023). Definitions, History, and Differentiating Characteristics of Shale Hydrocarbon Recovery. In M. Zeidouni (Ed.), *Shale Hydrocarbon Recovery* (pp. 1-9). Springer. https://doi.org/10.1007/978-3-031-23559-7

Zhang, B. W., Zhang, J. H., Feng, Z. H., Zeng, H. S., Huo, Q. L., & Zhang, K. (2021). Geological Conditions and Resource Potential for the Formation of Light Crude Oil from Gulong Shale in Qingshankou Formation, Songliao Basin. *Acta Petrolei Sinica, 42,* 1625-1639.

Zou, C. N., Zhao, Q., Zhang, G. S., & Xiong, B. (2016). Energy Revolution: From a Fossil Energy Era to a New Energy Era. *Natural Gas Industry B, 3,* 1-11. https://doi.org/10.1016/j.ngib.2016.02.001